Exploration of Drug Science

Open Exploration

Open Access Review

Technetium-99m-labeled peptides and their applications in radio imaging: advancements in Latin American research

Vaezeh Fathi Vavsari*, Saeed Balalaie*

Peptide Chemistry Research Institute, K. N. Toosi University of Technology, Tehran 1996715433, Iran

***Correspondence:** Vaezeh Fathi Vavsari, v.fathi83@yahoo.com; Saeed Balalaie, balalaie@kntu.ac.ir. Peptide Chemistry Research Institute, K. N. Toosi University of Technology, Tehran 1996715433, Iran

Academic Editor: Fanny Guzmán Quimbayo, Pontifical Catholic University of Valparaíso, Chile
Received: August 26, 2024 **Accepted:** October 25, 2024 **Published:** November 20, 2024

Cite this article: Fathi Vavsari V, Balalaie S. Technetium-99m-labeled peptides and their applications in radio imaging: advancements in Latin American research. Explor Drug Sci. 2024;2:814–35. https://doi.org/10.37349/eds.2024.00075

Abstract

A very new and highly specialized category of radiotracers that is still growing is radiolabeled peptides. Radiolabeled peptides, or radiopeptides, are powerful elements for diagnostic imaging and radionuclide therapy. These laboratory-manufactured peptides have gained attention due to their unique properties. The tiny structure of these peptides compared to proteins and antibodies makes them favorable regarding their availability through simple synthesis from amino acids, easy uptake by receptors on cancer cells, and high specificity and affinity for high-quality and accurate radio imaging. This study highlighted the potential of technetium-99m-labeled peptides in advancing diagnostic capabilities in directed research in Latin America.

Keywords

Technetium-99m, peptide, solid phase synthesis, imaging, radio imaging

Introduction

In the early 2010s, Bolzati et al. [1, 2] reviewed the development of technetium-99m (^{99m}Tc)-labeled radiopharmaceuticals, especially radiopeptides, in terms of their usage in radiotherapy and tumor imaging. The metastable nuclear isomer of Tc, ^{99m}Tc, has a half-life ($T_{½}$) of 6 h and emits gamma rays with 140 keV photon energy. The energy of ^{99m}Tc rays is sufficient to penetrate the biological tissues, however, the extremely short $T_{½}$ of ^{99m}Tc makes it impossible to store or transport it. Meanwhile, producing this radionuclide through bombardment of ^{100}Mo in cyclotrons is not preferred [3], because it yields the undesired ^{99g}Tc. Indeed, the development of ^{99m}Tc generators has been crucial for widespread clinical use, which uses the parent ^{99}Mo nuclide ($T_{½}$ of 66 h) obtained from highly enriched uranium [4, 5]. Correspondingly, the nuclear features of ^{99m}Tc make it perfect for use in diagnostic nuclear medicine [6]. Due to its artificial and metallic nature, a pharmacophore should be attached to chelating groups to construct ^{99m}Tc-labeled radiopharmaceuticals. The pharmacophore group plays a critical role in targeting specific tissues during imaging. Furthermore, the selected chelating group must be highly reactive toward

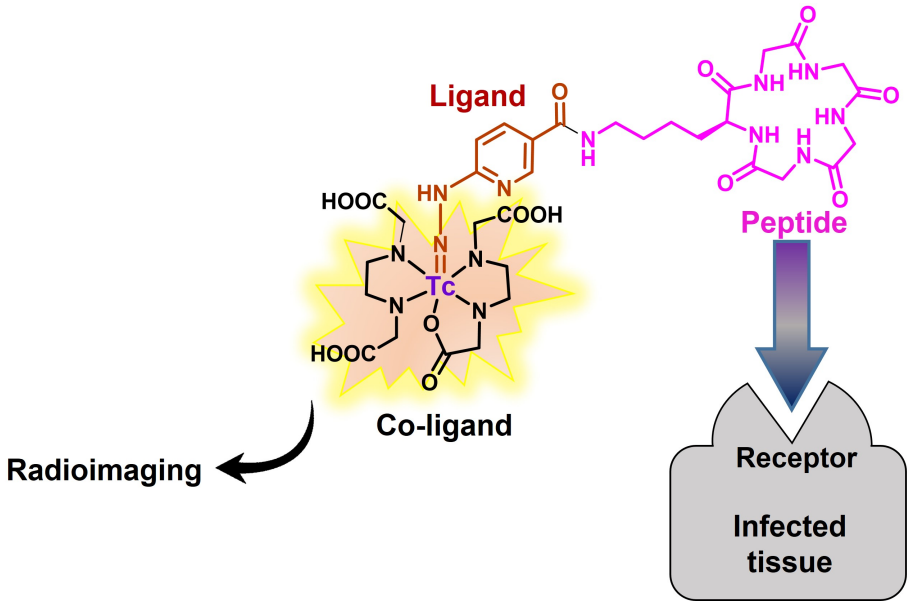

Graphical abstract. Technetium-99m-labeled peptides used in radio imaging

^{99m}Tc to construct an extremely stable complex [7]. In the published minireview in 2019, Miranda et al. [8] explored the radiochemical quality control of ^{99m}Tc-radiopharmaceuticals. They focused on optimizing chromatographic systems for assessing the radiochemical purity (RCP) of ^{99m}Tc-eluate and radiopharmaceuticals. Recently, Duatti [6] listed the development of ^{99m}Tc-based radio imaging using single photon emission tomography (SPECT). The focus of this literature study is on the synthesis, complexation, purification, and application of various ^{99m}Tc-radiopharmaceuticals [6].

In the emerging arena of nuclear imaging, diagnosis, and therapy, peptides are now essential motifs for in vivo targeting, radio imaging, monitoring, and visualization of infected tissues for the diagnosis and treatment of diseases [9–12]. Furthermore, radiolabeled peptides can identify the overexpressed peptide-binding receptors in many malignant cells and tumors [13, 14]. Besides, there are several benefits to employing peptides as bioactive molecules in radiolabeled detectors, including low adverse effects due to the low toxicity of peptides in comparison with the other pharmacophore compounds, great affinity for the target receptors, and the ability to incorporate hydrophilic functional groups into their structure to increase excretion and decrease lipophilicity [15–17]. Decreasing lipophilicity in a radiopharmaceutical leads to rapid renal excretion rather than intestinal clearance. Moreover, high tumor-to-background ratios are obtained by radiolabeled peptides, which is a crucial factor in radio imaging to achieve effective cancer-targeting and high-quality images [18, 19]. In 2020, Mohtavinejad et al. [20] discussed essential aspects of various radiolabeled peptides, including neurotensin (NT), somatostatin (SST), arginylglycylaspartic acid (RGD), exendin, vasoactive intestinal peptide, gastrin, and bombesin (BBN), in tumor imaging and pre-clinical and clinical phases of therapy. Another study collected recently published radiolabeled peptides, which were tested on imaging animals' organs [21].

Continuing our research on the synthesis of peptides, investigating their bioactivities, and their applicability in radio imaging [22–29], in this review we wanted to summarize the conducted studies in Latin American synthesis of special bioactive peptides, their complexation with ^{99m}Tc via special linkers and co-ligands, and their applicability in radio imaging and diagnosis of several diseases. This article covered various peptides, including BBN and its analogs, RGD peptides, NT, LyeTx I, and peptidoglycan aptamer.

^{99m}Tc-labeled peptides and their applications in radio imaging

The method of labeling peptides with ^{99m}Tc

^{99m}Tc is accessible in the 7^+ oxidation state by reducing $^{99m}TcO_4^-$ to a lower oxidation state using the stannous chloride. Ascorbic acid, as an antioxidant, is usually added to the solution of ^{99m}Tc complex to keep

it stable. The pH at which the complex is stable is 7.0 because it must be used in biological tissues. Then, Tc can tightly bind to a single specific atom or a small part of the chelating group. For instance, 2-hydrazinonicotinic acid (2-HYNIC), a bifunctional chelator suitable for Tc, easily attaches to bioactive molecules through an amidification reaction [30]. Since the coordination of HYNIC is possible from the nitrogen atom of its hydrazine moiety, it cannot saturate the coordination capacity of ^{99m}Tc, thus, the use of co-ligands is essential to complete the coordination sphere. Tricine, ethylenediaminediacetic acid (EDDA), nicotinic acid, pyridine dicarboxylic acid (PDA), glucamine, mannitol, and glucoheptonic acid are commonly used co-ligands to construct ^{99m}Tc-HYNIC complexes [31]. Figure 1 illustrates the process of binding HYNIC to a bioactive molecule and subsequently forming complexes with ^{99m}Tc using co-ligands. Studies showed that tricine and EDDA give the most stable radiochemical complex even up to one day post-incubation [32]. Therefore, HYNIC has been recently considered to bind to antibodies, fatty acids, proteins, and peptides via the formation of amide bonds, followed by coordinating with ^{99m}Tc to be used for radio imaging, diagnosing, and monitoring various targets and diseases, including activated T lymphocytes, pancreatic neuroendocrine neoplasms, cancer, and carcinoma cells [33–40].

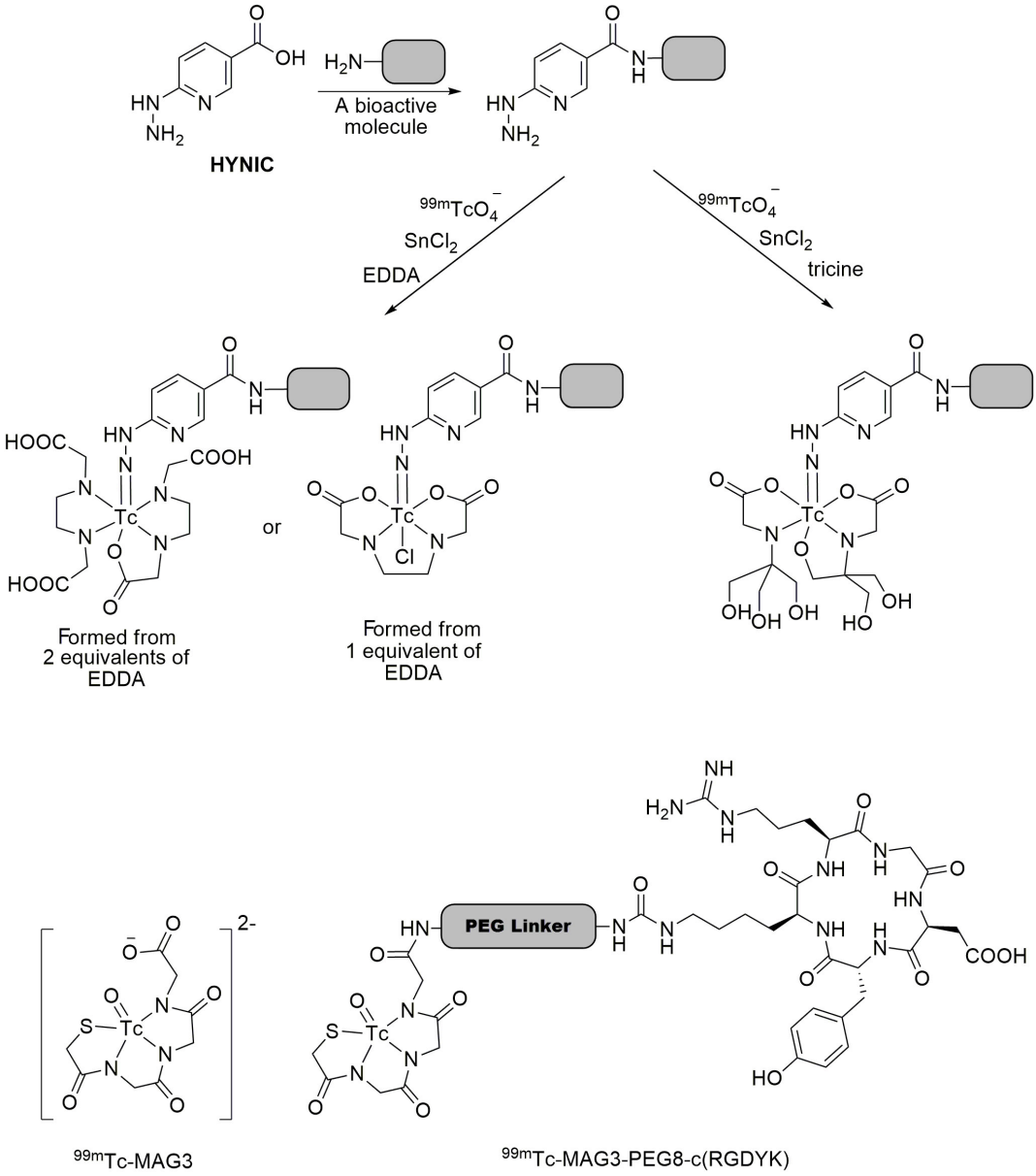

Figure 1. Synthesis of ^{99m}Tc-HYNIC complexes. The mentioned bioactive molecule can be any biologically active compound that has an amino group. ^{99m}Tc: technetium-99m; EDDA: ethylenediaminediacetic acid; HYNIC: hydrazinonicotinic acid; MAG3: mercaptoacetyltriglycine

^{99m}Tc-labeled BBN in detection of tumor cells

BBN is a 14-amino-acid peptide (pGlu-Gly-Arg-Leu-Gly-Thr-Gln-Trp-Ala-Val-Gly-His-Leu-Met-NH_2) that binds to G protein-coupled receptors (GPRs). The latter is overexpressed in different kinds of human cancer cells, especially breast, lung, and prostate cancers (PCs) [41]. Faintuch et al. [42] prepared a series of ^{99m}Tc-HYNIC-linker-BBN to compare their biodistribution and scintigraphy imaging in mice bearing PC-3 tumor cells. They found that ^{99m}Tc-HYNIC-βAla-BBN is rapidly produced during the radiolabeling step with no need for purification, bears high radiochemical efficiency with more with internalization (12% within 30 min) and tumor uptake [32, 42–44]. Inspired by the mentioned research, de Barros et al. [45] prepared a pH-sensitive liposome encapsulating ^{99m}Tc-HYNIC-βAla-$BBN_{(7-14)}$ and used it to detect human breast cancer. The prepared nano-liposome with an approximately 165 nm diameter displayed a strong signal in the tumor tissue, showing a good tumor-to-muscle of 9.31% injected dose (ID)/g. It was also enclosed that ^{99m}Tc-HYNIC-βAla-$BBN_{(7-14)}$ can recognize Capan-1 pancreatic adenocarcinoma at its early stage with an uptake of 0.47% ID/g [46], and LNCaP prostate tumor [47]. Another research revealed the applicability of ^{99m}Tc-HYNIC-BBN or imaging women's breasts with malignant tumors [48]. Later, Faintuch et al. [49] could design a ^{99m}Tc-mercaptoacetyltriglycine (MAG3) complex coupled to BBN via a 6-aminohexanoic acid (6-Ahx) linker (^{99m}Tc-MAG3-Ahx-BBN). The RCP of this complex was approximately 96% at neutral pH, exhibiting high internalization (75% within 30 min) and great affinity for BBN receptors [49]. Following their research, Faintuch et al. [50] compared the ability of ^{99m}Tc-MAG3-Ahx-BBN and ^{99m}Tc-MAG3-Ahx-DUP1 to diagnose prostate carcinoma. DUP1 is a synthetic peptide (Phe-Arg-Pro-Asn-Arg-Ala-Gln-Asp-Tyr-Asn-Thr-Asn) with high affinity for DU-145 prostate and PC-3 cells [51]. The mentioned study demonstrated that the DUP1 tracer was more hydrophilic than the BBN one, with greater kidney uptake. However, due to its higher specificity to receptors of gastrin-releasing peptide, the BBN tracer displayed superior internalization (78%), while tumor uptake for both tracers was comparable [50]. Many other BBN-based ^{99m}Tc-radiotracers have been developed through similar protocols to improve stability and high uptake in target tissues [52–59]. Moreover, the focus of some research is on the preparation of multifunctional systems containing BBN-based ^{99m}Tc-radiotracers conjugated to the surface modified nanoparticles (NPs) with target-specific molecular recognition [60–64].

Pretargeting involves the use of high affinity and specificity biomarkers to obtain a high contrast of target to the background, improving the tumor-to-nontumor ratio [65–67]. Morpholino oligomers (MORFs) contain DNA bases in their scaffold attached to morpholine rings through phosphonodiamidite groups. These synthetic oligomers are widely employed for nuclear-pre-targeted imaging [68–72]. Since binding MORF to a carrier through a covalent bond is difficult, the utilization of streptavidin (SA) as a linker makes it easy to attach a biotinylated carrier to biotinylated MORF via simple mixing. Consequently, Faintuch et al. [73] prepared ^{99m}Tc-MAG3-cMORF as well as Biotin-βAla-BBN and Biotin-MORF and mixed them in the presence of SA to have a ^{99m}Tc-labeled nano-peptide to image lymph nodes bearing tumor cells.

^{99m}Tc-labeled analogs of SST

SST is a kind of cyclic peptide hormone, containing 14 or 28 amino acids, which plays its role in different ways, including interaction with G protein-coupled SST receptors to control cell proliferation, regulation of cellular functions, and inhibiting the release of other hormones, such as insulin and glucagon secretion [74–76]. The peptidases distributed in plasma and tissues rapidly degrade the natural SST, therefore, its highly short life (1–3 min) makes it useless in clinical cases [77]. Consequently, many analogs of SST have been developed regarding the clinical approaches. Lanreotide or somatuline is an SST-analogue octapeptide, containing 8 amino acids (D-Nal-Cys-Tyr-D-Trp-Lys-Val-Cys-Thr-NH_2) cyclized through a disulfide bond between two cysteine moieties. Lanreotide can manage the symptoms resulting from neuroendocrine-active tumors [78]. In the early 2000s, its ^{99m}Tc complex was considered to be used in radio imaging of neuroendocrine tumors. Consequently, ^{99m}Tc-lanreotide was prepared in a tartrate-phthalate buffer solution, containing maltose, glycine, and $SnCl_2$ solution, followed by the addition of ^{99m}Tc. This complex was stable for 6 h, mainly distributed in the gastrointestinal tract, showing its applicability in

radiodiagnosis [79]. However, the study of this complex was of interest only in those years and forgotten later.

Octreotide (OCT) and octreotate (TATE) are more attractive than lanreotide in radio imaging studies for the detection of unrespectable neuroendocrine tumors. To aim for this, Melo et al. [80] developed the synthesis of ^{99m}Tc-HYNIC-Tyr^3-OCT and ^{99m}Tc-HYNIC-Tyr^3-TATE (Figure 2) and investigated their biodistribution. They found fast blood clearance and high biodistribution of OCT and TATE in the pancreas, intestine, stomach, lung, and blood. The great uptake of these radio-drugs in the kidney and pancreas is due to the high density of SST receptors. Moreover, low uptake was observed in bones, liver, spleen, heart, brain, and thyroid [80, 81]. In another research, OCT was loaded on Au NPs coated with Lys^3-BBN or mannose (Figure 3). The prepared radio-agents were useful to detect sentinel lymph nodes [82, 83]. The time-consuming preparation of such loaded radio drugs is one of the drawbacks of this method, which limits its clinical application.

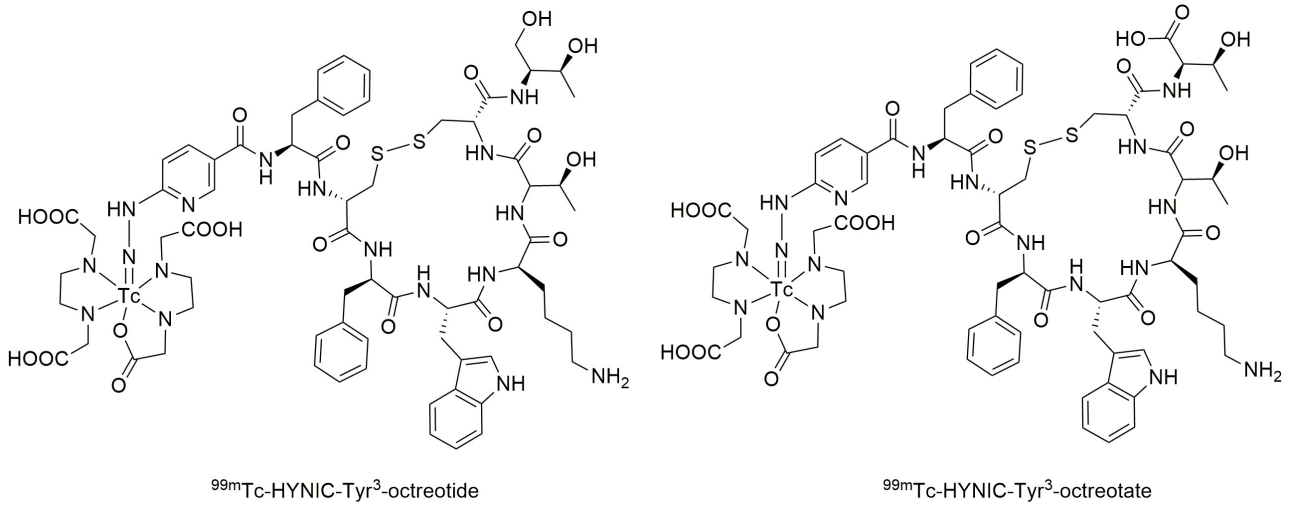

Figure 2. The structure of TATE and OCT. ^{99m}Tc: technetium-99m; HYNIC: hydrazinonicotinic acid; OCT: octreotide; TATE: octreotate

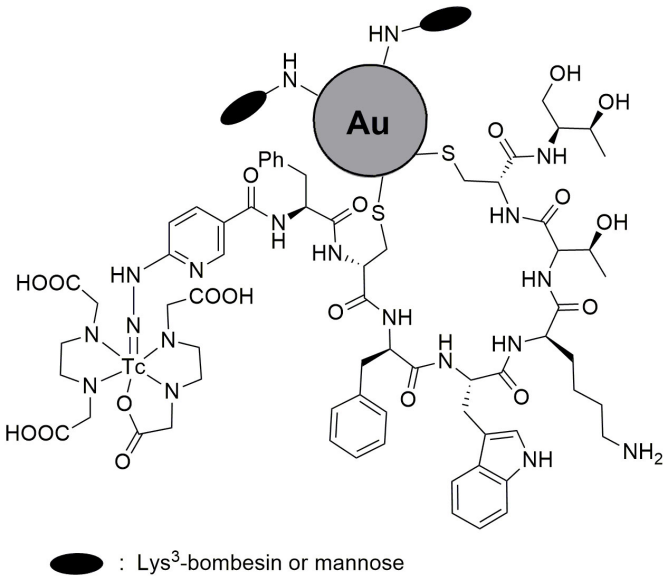

Figure 3. The loaded OCT on Au nanoparticles coated with Lys^3-bombesin or mannose. OCT: octreotide

^{99m}Tc-labeled exendin-4 fragment

Exendin-4 is an analog of glucagon-like peptide 1 (GLP-1), which can attach to GLP-1 receptors, expressed in patients who suffer from insulinomas, a kind of small pancreatic endocrine tumor [84–86]. Currently,

exendin-4 is consumed for the treatment of type 2 diabetes [87, 88]. Because radiolabeled exendin$_{(9-39)}$ has the potential to detect GLP-1 receptors and also OCT can identify SST receptors, a combination of HYNIC-exendin$_{(9-39)}$ and OCT (Figure 4) can detect malignant insulinomas pancreatic tumors, which express high and low densities of GLP-1 and SST receptors, respectively. Biodistribution studies of ^{99m}Tc-HYNIC-exendin$_{(9-39)}$-OCT showed suitable uptake in target tumor cells (2.71% ID/g), blood (1.5% ID/g), and kidney (95.0% ID/g) and it was rapidly eliminated from renal after 2 h [89–92].

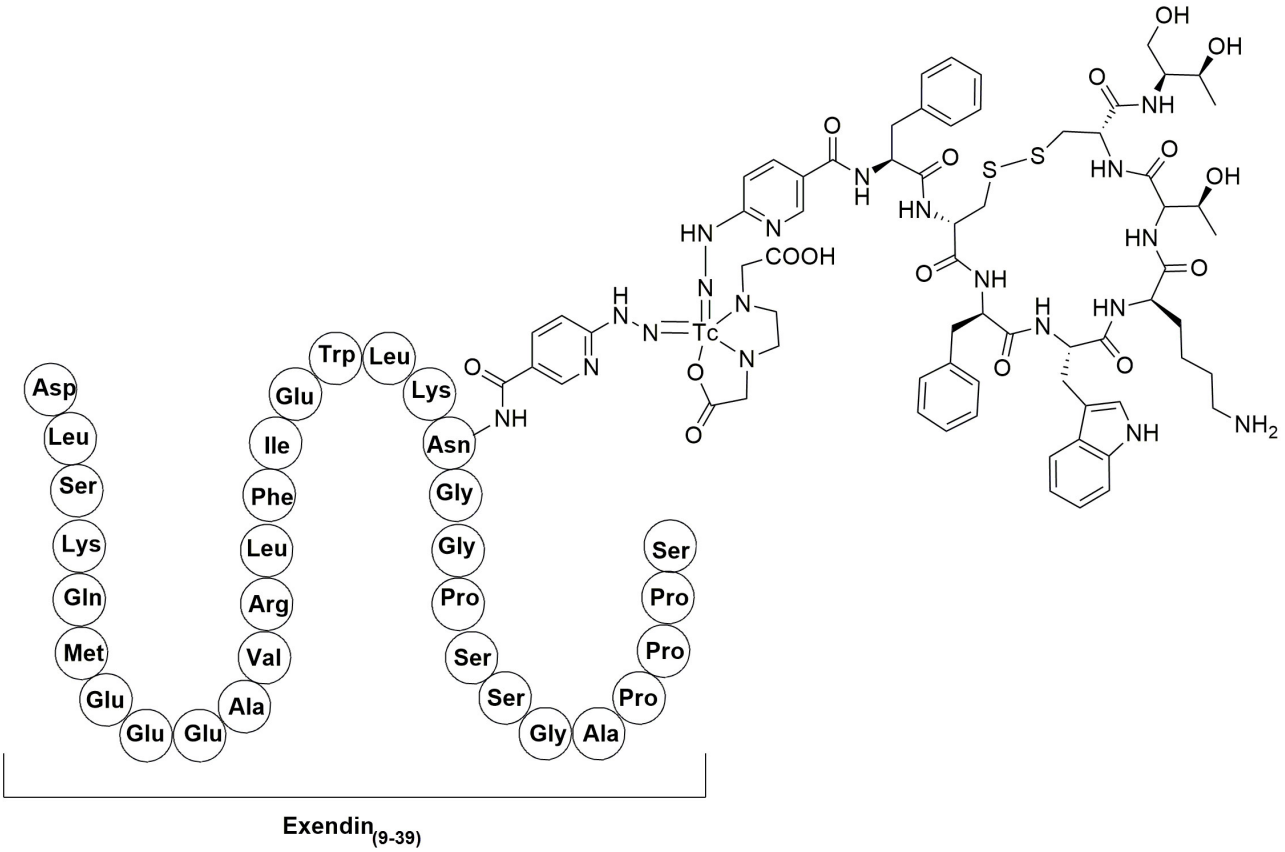

Figure 4. The structure of ^{99m}Tc-HYNIC-exendin$_{(9-39)}$-OCT. ^{99m}Tc: technetium-99m; HYNIC: hydrazinonicotinic acid; OCT: octreotide

^{99m}Tc-labeled RGD or RGD analogues

RGD is a tripeptide comprising Arg-Gly-Asp residue, which is responsible for cell adhesion to the extracellular matrix [93]. RGD peptides have the potential to be used in tissue engineering, therapy, and imaging [94, 95]. It has been validated that some kinds of cyclic peptides containing RGD residue can bind integrin $\alpha_v\beta_3$, which is linked to the progress of various diseases [96]. It must be noted that a cyclic RGD-pentapeptide, comprising of Arg-Gly-Asp-Tyr-Lys [c(RGDyK)], is a derivative of RGD with a high affinity for $\alpha_v\beta_3$ integrin, which is expressed on the cell membrane of many cancerous cells [97, 98]. Decristoforo et al. [99] synthesized c(RGDyK) to make ^{99m}Tc-HYNIC-c(RGDyK), as depicted in Figure 5. High uptake of the prepared radiotracer was observed in $\alpha_v\beta_3$-integrin-receptor-positive M21 melanoma cells up to 2.73% ID/g, while tumor-to-organ ratios were equivalent to that observed for [^{18}F]Galacto-RGD.

^{99m}Tc-MAG3 is frequently employed for renal and kidney function imaging [100, 101]. The carboxyl group of MAG3 can bind to a linker molecule, carrying a biomolecule. As shown in Figure 6, ^{99m}Tc-MAG3 is attached to c(RGDyK) via a polyethyleneglycol linker, forming ^{99m}Tc-MAG3-PEG8-c(RGDyK). It was revealed that ^{99m}Tc-MAG3-PEG8-c(RGDyK) traces malignant melanoma cells, SK-MEL-28, after 30 min of incubation with an internalization of 96.13%. Due to its specificity for human SK-MEL-28 cells, this radiotracer is efficient for the early diagnosis of melanoma [102, 103]. Moreover, this tracer was employed for imaging diverse tumor models, including blood, lungs, kidneys, spleen, stomach, pancreas, liver, intestine, muscle,

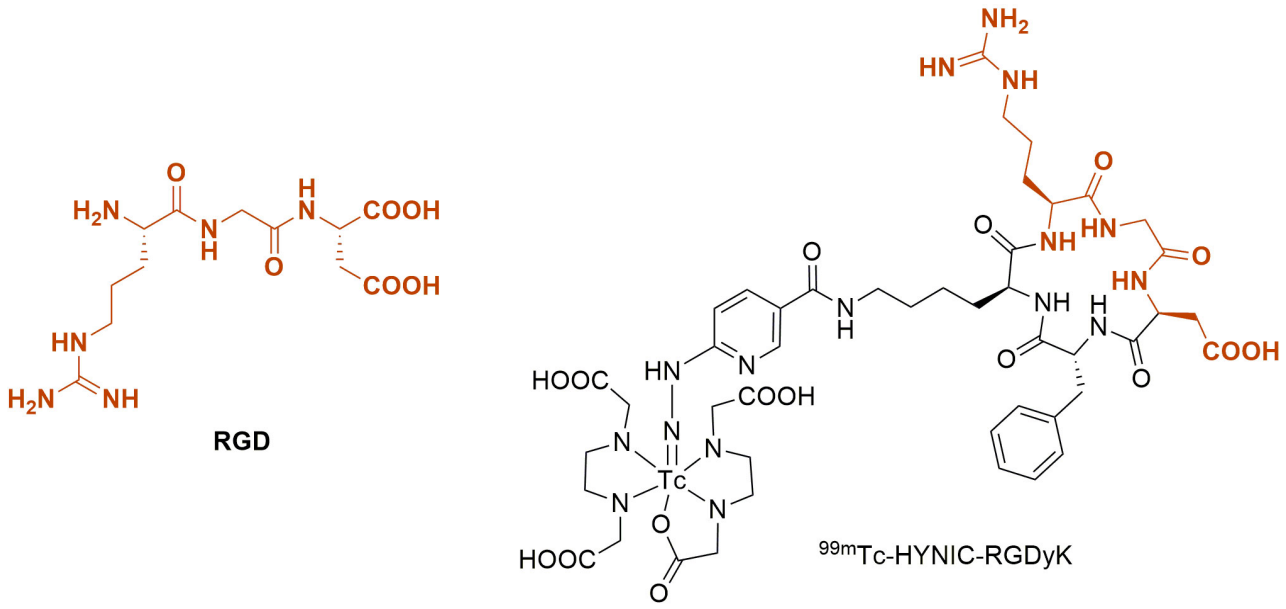

Figure 5. The structures of RGD tripeptide and ^{99m}Tc-HYNIC-RGDyK. ^{99m}Tc: technetium-99m; HYNIC: hydrazinonicotinic acid; RGD: arginylglycylaspartic acid

and bone carcinoma. The results revealed its high biodistribution in lung cancer cells, presenting the applicability of ^{99m}Tc-MAG3-PEG8-c(RGDyK) tracer to detect lung tumors in addition to melanoma cells [104]. It must be noted that polyethyleneglycol protects peptides from enzymatic degradation and thus decreases proteolysis, also increases overall hydrophilicity of the compound, leading to the increased peptide $T_{½}$ and stability [105]. Schiper et al. [106] prepared HYNIC-E-[c(RGDfK)]$_2$ (Figure 7) and made its complex with ^{99m}Tc to test its biodistribution on Swiss mice infected with osteonecrosis. This radiotracer showed the highest bone uptake after 15 days and could detect bone infarction efficiently [106]. In another research, c(RGDfK) was grafted on the surface of gold NPs modified with ^{99m}Tc-HYNIC-GGC, where GGC is Gly-Gly-Cys residue. This NP showed high specificity for detection of $\alpha_v\beta_3$-integrin-receptor-positive M21 melanoma cells [107].

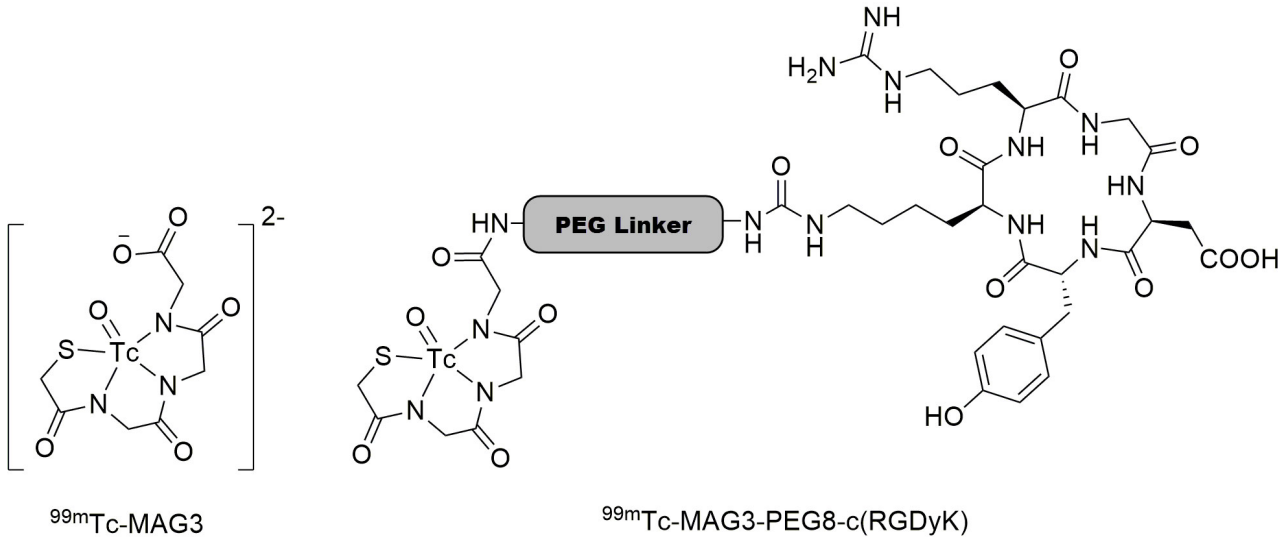

Figure 6. The structures of ^{99m}Tc-MAG3 and ^{99m}Tc-MAG3-PEG8-c(RGDyK). ^{99m}Tc: technetium-99m; MAG3: mercaptoacetyl-triglycine

Based on the previously published method [108, 109], Caporale et al. [110] synthesized a small cyclic pentapeptide of c(RGDfV), containing cyclized Arg-Gly-Asp-D-Phe-Val, which is an analogue of c(RGDyK). Then, two complexes of ^{99m}Tc-c(RGDfV) were prepared using nitrido nitrogen atoms (Figure 8). These complexes were stable after incubation for 4 h at 37°C in biological serum [110].

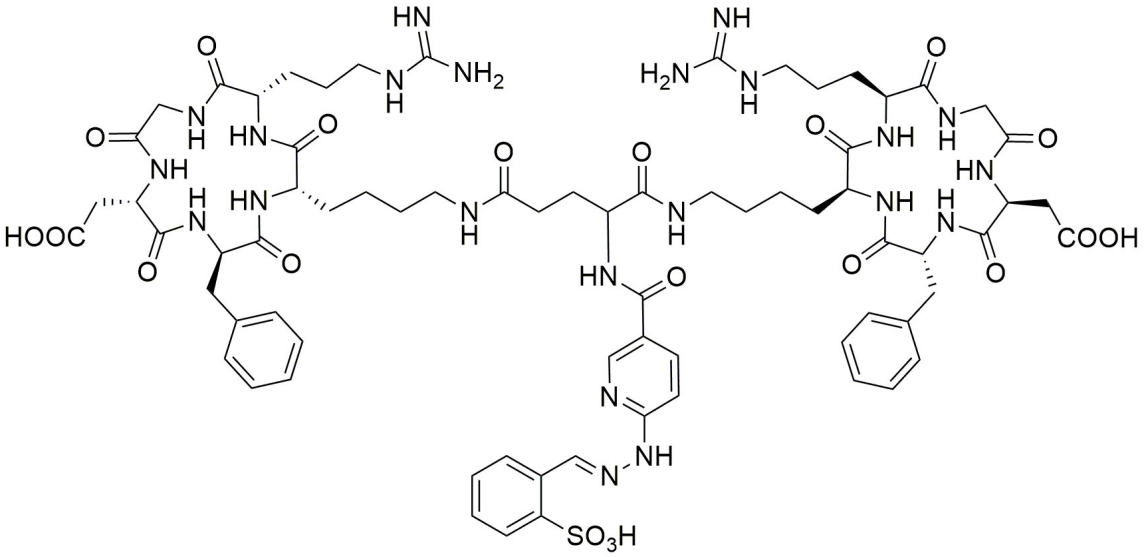

Figure 7. The structures of HYNIC-E-[c(RGDfK)]$_2$. HYNIC: hydrazinonicotinic acid

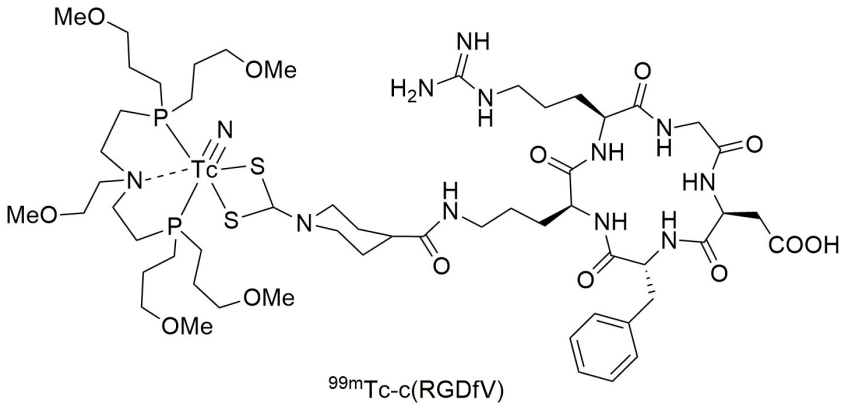

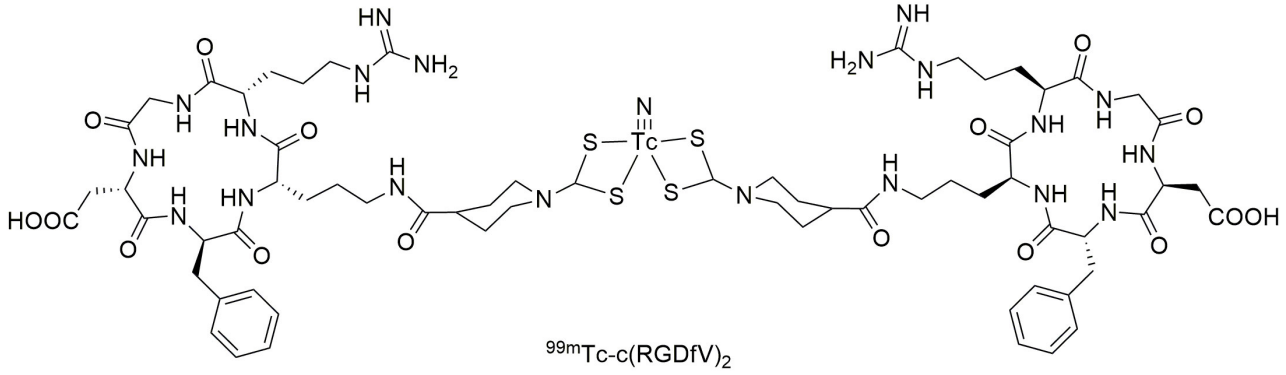

Figure 8. Two complexes of ^{99m}Tc-c(RGDfV)$_2$. ^{99m}Tc: technetium-99m

GX1 (Cys-Gly-Asn-Ser-Asn-Pro-Lys-Ser-Cys) is one of the high-affinity peptides with angiogenesis that can inhibit it. Accordingly, GX1 has been widely used for targeting and imaging cancer cells because of its binding specificity to integrin α3β1 receptors [111–113]. Correspondingly, binding the RGD peptide to GX1 may improve tumor cell affinity in radio imaging. In this regard, cyclized GX1 was introduced in two complexes with ^{99m}Tc, i.e. ^{99m}Tc-HYNIC-PEG4-c(GX1) and ^{99m}Tc-HYNIC-E-[c(RGDyK)-c(GX1)] (Figure 9). Both prepared tracers showed considerable stability after 4 h remaining in human serum under physiological conditions. They had great hydrophilic features with great renal excretion, however, the clearance of ^{99m}Tc-HYNIC-PEG4-c(GX1) from the blood was faster. After 5 min of incubation (0.41%), about 51% of the latter was internalized, while ^{99m}Tc-HYNIC-E-[c(RGDyK)-c(GX1)] showed the highest binding value after 2 h of incubation (0.35%). Comparable biodistribution was observed for both tracers in most

organs [114, 115]. Later, their ability in radio imaging was established, revealing better visualization, favoring tumor uptake (2.96% at 1 h), and highest binding (1.14%) at 2 h for ^{99m}Tc-HYNIC-E-[c(RGDyK)-c(GX1)] in glioma U87MG cells [116]. Moreover, magnetic resonance imaging (MRI) confirmed the specific binding of these tracers to human U87 glioblastoma in the brain [117]. Another research signified that a remarkable uptake can be obtained by injecting ^{99m}Tc-HYNIC-PEG4-c(GX1) into mice bearing B16F10 and SK-MEL-28 melanoma cells (1.41% and 2.42%, respectively) at 1 h [115].

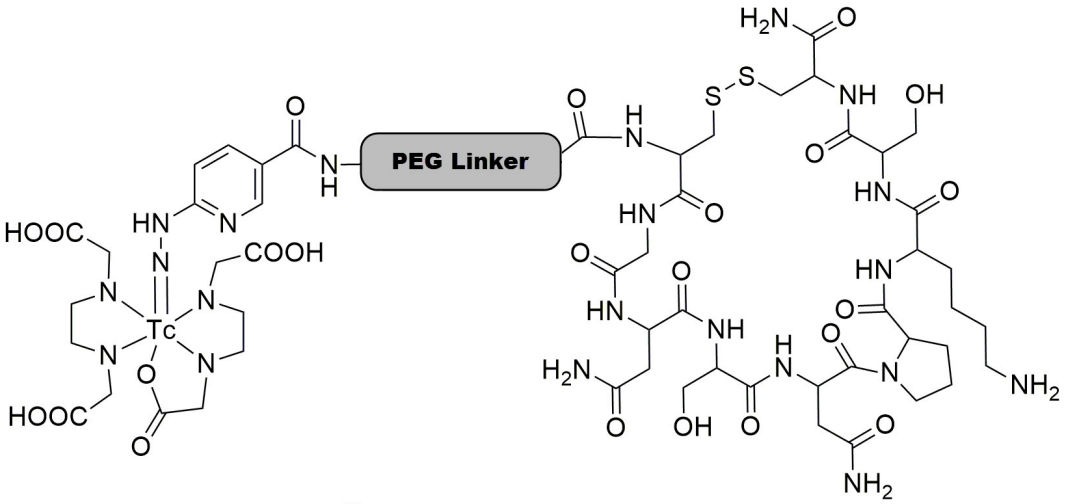

^{99m}Tc-HYNIC-PEG4-c(GX1)

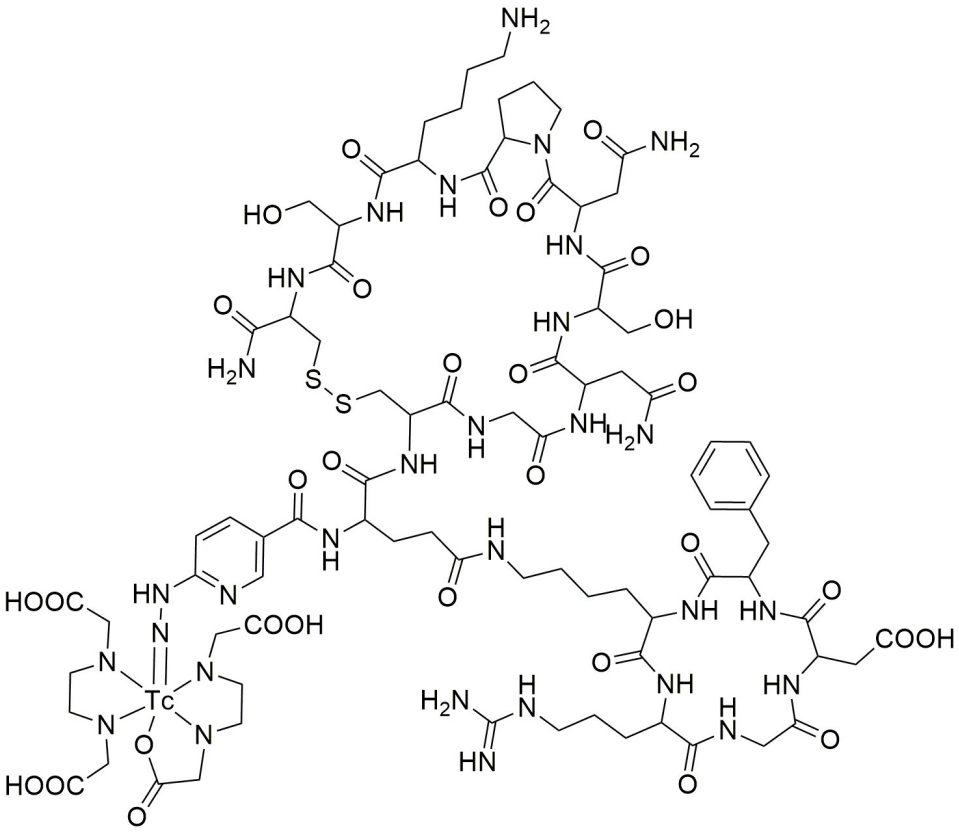

^{99m}Tc-HYNIC-E-[c(RGDyK)-c(GX1)]

Figure 9. Two complexes of ^{99m}Tc-HYNIC-PEG4-c(GX1) and ^{99m}Tc-HYNIC-E-[c(RGDyK)-c(GX1)]. ^{99m}Tc: technetium-99m; GX1: Cys-Gly-Asn-Ser-Asn-Pro-Lys-Ser-Cys; HYNIC: hydrazinonicotinic acid

In another study, a hexapeptide of Gly-Arg-Gly-Asp-His-Val (GRGDHV) was synthesized as an RGD analog, and labeled with a tricarbonyl complex of ^{99m}Tc, as illustrated in Figure 10. However, the sites of complexation of peptide with ^{99m}Tc have not been determined. This complex was stable for 24 h in human serum under biological conditions. Moreover, after 1 h of incubation, ^{99m}Tc(CO)$_3$-GRGDHV showed distinct binding in C6 tumorigenic cells with bound and internalized fractions of 22% and 34%, respectively. The accumulation of this radiopeptide was observed in the brains of glioblastoma allograft tumor-bearing rats and normal rats, showing biodistribution up to 1.57 and 0.6, respectively, at 4 h. The results showed promising application of this radiolabeled peptide in the clinical diagnosis of glioblastoma [118].

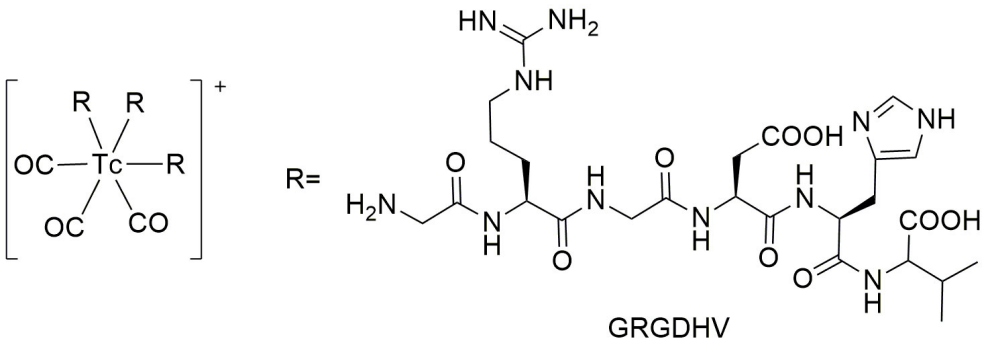

Figure 10. The structure of ^{99m}Tc(CO)$_3$-GRGDHV. ^{99m}Tc: technetium-99m; GRGDHV: Gly-Arg-Gly-Asp-His-Val

^{99m}Tc-labeled NT

NT is a neuropeptide, containing 13 amino acids of pyroGlu-Leu-Tyr-Glu-Asn-Lys-Pro-Arg-Arg-Pro-Tyr-Ile-Leu, playing its role in the central nervous system through interaction with dopamine receptors, smoothing muscle contraction, and regulation of luteinizing hormone and prolactin release [119–121]. Regarding the published results for the application of NT analogues in tumor imaging [122], Teodoro et al. [123] investigated the bioactivities of NT$_{(8–13)}$ analogue (Arg-NMe-Arg-Pro-Tyr-Ile-Leu) using its complex ^{99m}Tc-HYNIC-βAla-NT$_{(8–13)}$. Considerably high uptake of this tracer was observed for the lung, blood, and kidneys, while it was rapidly eliminated from the blood. Moreover, low uptake of this tracer was detected in the liver and intestine, showing its potential to be used in tumor imaging due to its high uptake and fast clearance from the blood [123].

^{99m}Tc-labeled antibacterial peptides

The cationic peptide LyeTx I is a natural 25 amino acid peptide, isolated from *Lycosa erythrognatha* venom, exhibiting antimicrobial activities [124–126]. Fuscaldi et al. [127] designed two chelating agents for ^{99m}Tc using C- and N-terminus of LyeTx I and HYNIC to give LyeTx I-K-HYNIC and HYNIC-LyeTx I, respectively. Then, the bioactivities of these agents were determined against *Staphylococcus aureus* and *Escherichia coli*, and it was discovered that the latter couldn't inhibit the growth of bacterium, while the former LyeTx I-K-HYNIC showed antibacterial properties with minimum inhibitory concentration (MIC) values of 5.05 μmol/L and 10.01 μmol/L against the mentioned species, respectively. Accordingly, ^{99m}Tc-LyeTx I-K-HYNIC complex was prepared with high purity to study infected tissues [127, 128]. In that study, researchers evaluated the biodistribution of two peptidoglycan aptamers, Antibac1 and Antibac2, which were labeled with ^{99m}Tc. These aptamers were specifically designed for bacterial infection diagnosis. The results exhibited that these tracers can easily recognize a bacterial infection focus [129].

Recently, ubiquitin (UBI) peptide is a cationic, synthetic antimicrobial peptide fragment. It has been considered a versatile antibacterial agent to be labeled with ^{99m}Tc [130–132], which is useful for distinguishing bacterial infections. The use of radiolabeled peptides for infection imaging in humans has been an area of active research. Here are some key findings from clinical studies involving ^{99m}Tc-UBI$_{(29–41)}$ as an infection-imaging agent [133]. In 2005, a 29–41 fragment of UBI with the sequence of Thr-Gly-Arg-Ala-Lys-Arg-Arg-Met-Gln-Tyr-Asn-Arg-Arg was labeled with ^{99m}Tc through coordination using its Lys and

Arg7 amino acids. The obtained ^{99m}Tc-UBI$_{(29–41)}$ was injected into patients with osteomyelitis, diabetes, and fever of unknown origin. Imaging showed infected tissues, which were comparable with the results obtained by biopsy [134–136]. In another research, it was determined that the imaging results of infected tissues obtained by ^{99m}Tc-UBI$_{(29–41)}$ were in agreement with those recorded by ^{67}Ga-citrate. Moreover, after 24 h, nearly 85% of ^{99m}Tc-UBI$_{(29–41)}$ is eliminated by renal clearance [137]. Vallejo et al. [138] used this radiotracer to detect mediastinitis after cardiac surgery. Furthermore, ^{99m}Tc-UBI$_{(29–41)}$ was applicable to diagnose musculoskeletal [139] and postsurgical spinal infections [140].

Discussion

Table 1 shows a summary of the peptide-^{99m}Tc complexes discussed in this review article. This table depicts their target cells, uptake amounts by the target, biodistribution of the complex in different organs, current applications, and advantages and usage of the prepared complexes.

Table 1. The summary of peptide-^{99m}Tc complexes in radio imaging

Entry	Peptide-^{99m}Tc complexes	Target cells or receptors	Uptake by target (% ID/g)	Biodistribution	Current applications	Advantages	Reference
1	^{99m}Tc-HYNIC-βAla-BBN$_{(7–14)}$	BBN-positive tumor cells, Capan-1 pancreatic adenocarcinoma	0.47–9.31	Tumors, spleen, the liver, and muscles	Imaging of breast tumors	Rapid clearance by renal excretion, higher uptake by tumors	[45, 46]
2	^{99m}Tc-MAG3-Ahx-DUP1	DU-145 prostate and PC-3 cells	1.23	Tumors, pancreas, spleen, lung, liver, and kidney	Diagnosis of prostate carcinoma	Rapid clearance	[50]
3	^{99m}Tc-MAG3-cMORF	PC-3 cells	2.58	Tumors, kidney, intestines, and liver	Imaging of lymph nodes bearing tumor cells	High tumor uptake	[73]
4	^{99m}Tc-lanreotide	Neuroendocrine-active tumors	Not determined	Intestine, kidney, lung, and liver	Imaging of neuroendocrine tumors	-	[79]
5	^{99m}Tc-HYNIC-Tyr^3-OCT	Somatostatin receptors	1.65–19.12	Pancreas, intestine, stomach, lung, and blood	Imaging of sentinel lymph nodes	High somatostatin receptor uptake	[80, 81]
6	^{99m}Tc-HYNIC-Tyr^3-octreotate	Somatostatin receptors	1.0–26.0	Pancreas, intestine, stomach, lung, and blood	Imaging of sentinel lymph nodes	High somatostatin receptor uptake	[80, 81]
7	^{99m}Tc-HYNIC-exendin$_{(9–39)}$-OCT	GLP-1 receptors	2.71	Tumors, blood, and kidney	Detection of malignant insulinomas pancreatic tumors	Rapid clearance	[89–92]
8	^{99m}Tc-HYNIC-c(RGDyK)	$\alpha_v\beta_3$-integrin-receptor-positive M21 melanoma cells	2.73	Tumors, intestine, and kidney	Imaging of integrin $\alpha_v\beta_3$ in coronary arterial and peripheral vascular angiogenesis	Low blood retention, low liver, and muscle uptakes	[99]
9	MAG3-PEG8-c(RGDyK)	SK-MEL-28 cells	7.85	Tumors, intestine, liver, and kidney	Early diagnosis of malignant melanoma	Stable internalization until 120 min	[102, 103]
10	^{99m}Tc-HYNIC-E-[c(RGDfK)]$_2$	Severely devascularized bone	4.2	Bone	Imaging of osteonecrosis	Remarkable renal excretion	[105]
11	^{99m}Tc-HYNIC-GGC-Au NPs	$\alpha_v\beta_3$-integrin-receptor-positive M21 melanoma cells	8.18	Tumors, pancreas, liver, and kidney	Imaging of tumor $\alpha_v\beta_3$ expression	High spatial resolution	[106]

Table 1. The summary of peptide-^{99m}Tc complexes in radio imaging (*continued*)

Entry	Peptide-^{99m}Tc complexes	Target cells or receptors	Uptake by target (% ID/g)	Biodistribution	Current applications	Advantages	Reference
12	^{99m}Tc-HYNIC-PEG4-c(GX1)	Glioma U87MG cells	1.52	Tumors, blood, liver, kidney, and intestines	Targeting angiogenesis in glioma tumors	-	[113–115]
13	^{99m}Tc-HYNIC-E-[c(RGDyK)-c(GX1)]	Glioma U87MG cells	2.96	Tumors, blood, liver, kidney, and intestines	Targeting angiogenesis in glioma tumors	Great renal excretion	[113–115]
14	^{99m}Tc$(CO)_3$-GRGDHV	C6 tumorigenic cells	1.57	Brain, heart, spleen, lung, liver, and kidney	Imaging of tumor $\alpha_v\beta_3$ expression	Hydrophilic character	[117, 118]
15	^{99m}Tc-HYNIC-βAla-$NT_{(8–13)}$	Tumor cells	> 18.1	Tumors, lung, blood, and kidneys	Tumor imaging	Low uptake in liver and intestine, high uptake, and fast clearance from the blood	[122, 123]
16	^{99m}Tc-LyeTx I-K-HYNIC	Bacterial infection	-	Not determined	Infection imaging	-	[128]
17	^{99m}Tc-$UBI_{(29–41)}$	Infected tissues	-	Not determined	Diagnosis of musculoskeletal and postsurgical spinal infections	-	[136–139]

-: no data. ^{99m}Tc: technetium-99m; Ahx: aminohexanoic acid; BBN: bombesin; GLP-1: glucagon-like peptide 1; GRGDHV: Gly-Arg-Gly-Asp-His-Val; GX1: Cys-Gly-Asn-Ser-Asn-Pro-Lys-Ser-Cys; HYNIC: hydrazinonicotinic acid; ID: injected dose; MAG3: mercaptoacetyltriglycine; MORF: morpholino oligomer; NPs: nanoparticles; NT: neurotensin; OCT: octreotide; PC-3: prostate cancer-3

Conclusions

Radio imaging is an essential technique to monitor and diagnose a wide variety of diseases, including cancer, Alzheimer's, and infections. The emission of gamma rays with a $T_{½}$ of 6 h and 140 keV photon energy makes ^{99m}Tc a valuable metastable nuclear isomer to be used in SPECT. To this aim, ^{99m}Tc is tightly binding to a chelating group, such as HYNIC, and co-ligands. The use of ^{99m}Tc-labeled peptides for tumor imaging has gained significant attention in clinical research. These radiolabeled peptides offer advantages such as high specificity, favorable pharmacokinetics, and minimal radiation exposure. The chelating group is attached to a bioactive molecule, which possesses affinity for a specific receptor. In this review, we showed different kinds of bioactive peptides labeled with ^{99m}Tc, which are useful in the clinical detection of prostate, pancreas, lung, and stomach tumors. The application of ^{99m}Tc-labeled antibacterial peptides holds promise for detecting infected tissues and tracing bacterial function. In summary, ^{99m}Tc-labeled peptides hold promise for non-invasive disease imaging, and ongoing research aims to improve their clinical impact.

Abbreviations

2-HYNIC: 2-hydrazinonicotinic acid

6-Ahx: 6-aminohexanoic acid

^{99m}Tc: technetium-99m

BBN: bombesin

EDDA: ethylenediaminediacetic acid

GLP-1: glucagon-like peptide 1

GRGDHV: Gly-Arg-Gly-Asp-His-Val

GX1: Cys-Gly-Asn-Ser-Asn-Pro-Lys-Ser-Cys

ID: injected dose

MAG3: mercaptoacetyltriglycine

MORFs: morpholino oligomers

NPs: nanoparticles

NT: neurotensin

OCT: octreotide

PCs: prostate cancers

RCP: radiochemical purity

RGD: arginylglycylaspartic acid

SA: streptavidin

SPECT: single photon emission tomography

SST: somatostatin

$T_{½}$: half-life

TATE: octreotate

UBI: ubiquitin

Declarations

Acknowledgments

We gratefully acknowledge Iran National Science Foundation (INSF, grant no 99029802) for the financial support.

Author contributions

VFV: Conceptualization, Investigation, Writing—original draft, Writing—review & editing. SB: Conceptualization, Investigation, Writing—original draft, Writing—review & editing, Funding acquisition.

Conflicts of interest

Both authors declare that they have no conflicts of interest.

Ethical approval

Not applicable.

Consent to participate

Not applicable.

Consent to publication

Not applicable.

Availability of data and materials

Not applicable.

Funding

This study was funded by Iran National Science Foundation (INSF) [99029802]. The funder had no role in study design, data collection and analysis, decision to publish, or preparation of the manuscript.

References

1. Bolzati C, Refosco F, Marchiani A, Ruzza P. 99mTc-radiolabelled peptides for tumour imaging: present and future. Curr Med Chem. 2010;17:2656–83. [DOI] [PubMed]
2. Bolzati C, Carta D, Salvarese N, Refosco F. Chelating systems for 99mTc/188Re in the development of radiolabeled peptide pharmaceuticals. Anticancer Agents Med Chem. 2012;12:428–61. [DOI] [PubMed]
3. Beaver J, Hupf H. Production of 99mTc on a medical cyclotron: a feasibility study. J Nucl Med. 1971; 12:739–41.
4. Brown MA, Johnson N, Gelis AV, Stika M, Servis AG, Bakken A, et al. Recovery of high specific activity molybdenum-99 from accelerator-induced fission on low-enriched uranium for technetium-99m generators. Sci Rep. 2021;11:13292. [DOI] [PubMed] [PMC]
5. Lee SK, Beyer GJ, Lee JS. Development of Industrial-Scale Fission ^{99}Mo Production Process Using Low Enriched Uranium Target. Nucl Eng Technol. 2016;48:613–23. [DOI]
6. Duatti A. Review on ^{99m}Tc radiopharmaceuticals with emphasis on new advancements. Nucl Med Biol. 2021;92:202–16. [DOI] [PubMed]
7. Liu S. Bifunctional coupling agents for radiolabeling of biomolecules and target-specific delivery of metallic radionuclides. Adv Drug Deliv Rev. 2008;60:1347–70. [DOI] [PubMed] [PMC]
8. Miranda ACC, Durante ACR, Fuscaldi LL, de Barboza MF. Current Approach in Radiochemical Quality Control of the ^{99m}Tc-Radiopharmaceuticals: a mini-review. Braz Arch Biol Technol. 2019;62: e19180545. [DOI]
9. Zanzonico P. An overview of nuclear imaging. Radiopharm Chem. 2019:101–17. [DOI]
10. Hamoudeh M, Kamleh MA, Diab R, Fessi H. Radionuclides delivery systems for nuclear imaging and radiotherapy of cancer. Adv Drug Deliv Rev. 2008;60:1329–46. [DOI] [PubMed]
11. Vivier D, Sharma SK, Zeglis BM. Understanding the in vivo fate of radioimmunoconjugates for nuclear imaging. J Labelled Comp Radiopharm. 2018;61:672–92. [DOI] [PubMed]
12. Polvoy I, Flavell RR, Rosenberg OS, Ohliger MA, Wilson DM. Nuclear Imaging of Bacterial Infection: The State of the Art and Future Directions. J Nucl Med. 2020;61:1708–16. [DOI] [PubMed] [PMC]
13. Vāvere AL, Rossin R. Molecular imaging of cancer with radiolabeled peptides and PET. Anticancer Agents Med Chem. 2012;12:462–75. [DOI] [PubMed]
14. Rezazadeh F, Sadeghzadeh N. Tumor targeting with ^{99m}Tc radiolabeled peptides: Clinical application and recent development. Chem Biol Drug Des. 2019;93:205–21. [DOI] [PubMed]
15. Okarvi SM. Peptide-based radiopharmaceuticals: future tools for diagnostic imaging of cancers and other diseases. Med Res Rev. 2004;24:357–97. [DOI] [PubMed]
16. Richter S, Wuest F. ^{18}F-Labeled Peptides: The Future Is Bright. Molecules. 2014;19:20536–56. [DOI] [PubMed] [PMC]
17. Liu Y, Welch MJ. Nanoparticles labeled with positron emitting nuclides: advantages, methods, and applications. Bioconjug Chem. 2012;23:671–82. [DOI] [PubMed] [PMC]
18. Desai P, Rimal R, Sahnoun SEM, Mottaghy FM, Möller M, Morgenroth A, et al. Radiolabeled Nanocarriers as Theranostics—Advancement from Peptides to Nanocarriers. Small. 2022;18: e2200673. [DOI] [PubMed]
19. Rangger C, Haubner R. Radiolabelled Peptides for Positron Emission Tomography and Endoradiotherapy in Oncology. Pharmaceuticals (Basel). 2020;13:22. [DOI] [PubMed] [PMC]
20. Mohtavinejad N, Shafiee Ardestani M, Khalaj A, Pormohammad A, Najafi R, Bitarafan-Rajabi A, et al. Application of radiolabeled peptides in tumor imaging and therapy. Life Sci. 2020;258:118206. [DOI] [PubMed]
21. Kręcisz P, Czarnecka K, Królicki L, Mikiciuk-Olasik E, Szymański P. Radiolabeled Peptides and Antibodies in Medicine. Bioconjug Chem. 2021;32:25–42. [DOI] [PubMed] [PMC]

22. Talaei B, Fathi Vavsari V, Balalaie S, Arabanian A, Bijanzadeh HR. Synthesis of Novel Peptides Using Unusual Amino Acids. Iran J Pharm Res. 2020;19:370–82. [DOI] [PubMed] [PMC]
23. Fathi V, Ramezanpour S, Balalaie S, Rominger F, Bijanzadeh HR. An Efficient Approach to the Synthesis of Hydrazinyl *Pseudo*-Peptides. Helv Chim Acta. 2014;97:1630–7. [DOI]
24. Haji Abbasi Somehsaraie M, Fathi Vavsari V, Kamangar M, Balalaie S. Chemical Wastes in the Peptide Synthesis Process and Ways to Reduce Them. Iran J Pharm Res. 2022;21:e123879. [DOI] [PubMed] [PMC]
25. Fathi Vavsari V, Balalaie S. An overview on the two recent decades' study of peptides synthesis and biological activities in Iran. J Iran Chem Soc. 2022;19:331–51. [DOI]
26. Hatamabadi D, Joukar S, Shakeri P, Balalaie S, Yazdani A, Khoramjouy M, et al. Synthesis and Radiolabeling of Glu-Urea-Lys with ^{99m}Tc-Tricarbonyl-Imidazole-Bathophenanthroline Disulfonate Chelation System and Biological Evaluation as Prostate-Specific Membrane Antigen Inhibitor. Cancer Biother Radiopharm. 2023;38:486–96. [DOI] [PubMed]
27. Sheikhhosseini E, Balalaie S, Bigdeli M. Synthesis of Nocistatin C-terminal and it's Amide Derivatives as an Opioid Peptide. Iran J Pharm Res. 2016;15:337–42. [PubMed] [PMC]
28. Namjoo M, Ghafouri H, Assareh E, Aref AR, Mostafavi E, Hamrahi Mohsen A, et al. A VEGFB-Based Peptidomimetic Inhibits VEGFR2-Mediated PI3K/Akt/mTOR and PLCγ/ERK Signaling and Elicits Apoptotic, Antiangiogenic, and Antitumor Activities. Pharmaceuticals (Basel). 2023;16:906. [DOI] [PubMed] [PMC]
29. Khosravi H, Ghazvini HJ, Kamangar M, Rominger F, Balalaie S. Migratory cycloisomerization of 1,3-dien-5-ynes conjugated with pseudopeptides in assembly of benzo[7]annulenes. Chem Commun (Camb). 2022;58:2164–7. [DOI] [PubMed]
30. Meszaros LK, Dose A, Biagini SCG, Blower PJ. Hydrazinonicotinic acid (HYNIC) – Coordination chemistry and applications in radiopharmaceutical chemistry. Inorg Chim Acta. 2010;363:1059–69. [DOI]
31. Ono M, Arano Y, Mukai T, Fujioka Y, Ogawa K, Uehara T, et al. ^{99m}Tc-HYNIC-derivatized ternary ligand complexes for ^{99m}Tc-labeled polypeptides with low *in vivo* protein binding. Nucl Med Biol. 2001;28:215–24. [DOI] [PubMed]
32. Faintuch BL, Santos RLSR, Souza ALFM, Hoffman TJ, Greeley M, Smith CJ. ^{99m}Tc-HYNIC-Bombesin (7-14)NH_2: Radiochemical Evaluation with Co-ligands EDDA (EDDA = Ethylenediamine-N,N′-diacetic Acid), Tricine, and Nicotinic Acid. Synth React Inorg Met Org Nano Met Chem. 2005;35:43–51. [DOI]
33. Xu J, Li Y, Xu X, Zhang J, Zhang Y, Yu X, et al. Clinical application of ^{99m}Tc-HYNIC-TOC SPECT/CT in diagnosing and monitoring of pancreatic neuroendocrine neoplasms. Ann Nucl Med. 2018;32:446–52. [DOI] [PubMed]
34. Isaac-Olivé K, Ocampo-García BE, Aranda-Lara L, Santos-Cuevas CL, Jiménez-Mancilla NP, Luna-Gutiérrez MA, et al. [^{99m}Tc-HYNIC-*N*-dodecylamide]: a new hydrophobic tracer for labelling reconstituted high-density lipoproteins (rHDL) for radioimaging. Nanoscale. 2019;11:541–51. [DOI] [PubMed]
35. Wu Y, Li L, Wang Z, Shi J, Hu Z, Gao S, et al. Imaging and monitoring HER2 expression in breast cancer during trastuzumab therapy with a peptide probe ^{99m}Tc-HYNIC-H10F. Eur J Nucl Med Mol Imaging. 2020;47:2613–23. [DOI] [PubMed]
36. Blankenberg FG, Backer MV, Levashova Z, Patel V, Backer JM. In vivo tumor angiogenesis imaging with site-specific labeled ^{99m}Tc-HYNIC-VEGF. Eur J Nucl Med Mol Imaging. 2006;33:841–8. [DOI] [PubMed]
37. Loose D, Vermeersch H, De Vos F, Deron P, Slegers G, Van de Wiele C. Prognostic value of ^{99m}Tc-HYNIC annexin-V imaging in squamous cell carcinoma of the head and neck. Eur J Nucl Med Mol Imaging. 2008;35:47–52. [DOI] [PubMed]

38. Rezaeianpour S, Bozorgi AH, Moghimi A, Almasi A, Balalaie S, Ramezanpour S, et al. Synthesis and Biological Evaluation of Cyclic [^{99m}Tc]-HYNIC-CGPRPPC as a Fibrin-Binding Peptide for Molecular Imaging of Thrombosis and Its Comparison with [^{99m}Tc]-HYNIC-GPRPP. Mol Imaging Biol. 2017;19: 256–64. [DOI] [PubMed]
39. Sun H, Jiang XF, Wang S, Chen HY, Sun J, Li PY, et al. ^{99m}Tc-HYNIC-TOC scintigraphy in evaluation of active Graves' ophthalmopathy (GO). Endocrine. 2007;31:305–10. [DOI] [PubMed]
40. Mathur A, Sharma AK, Murhekar VV, Mallia MB, Pawade S, Sarma HD, et al. Syntheses and biological evaluation of ^{99m}Tc-HYNIC-fatty acid complexes for myocardial imaging. RSC Adv. 2015;5:93374–85. [DOI]
41. Mansi R, Minamimoto R, Mäcke H, Iagaru AH. Bombesin-Targeted PET of Prostate Cancer. J Nucl Med. 2016;57:67S–72S. [DOI] [PubMed]
42. Faintuch BL, Teodoro R, Duatti A, Muramoto E, Faintuch S, Smith CJ. Radiolabeled bombesin analogs for prostate cancer diagnosis: preclinical studies. Nucl Med Biol. 2008;35:401–11. [DOI]
43. Fuscaldi LL, de Barros ALB, Santos CRP, de Souza CM, Cassali GD, de Oliveira MC, et al. Evaluation of the optimal LNCaP prostate tumour developmental stage to be assessed by ^{99m}Tc-HYNIC-βAla-Bombesin$_{(7-14)}$ in an experimental model. J Radioanal Nucl Chem. 2014;300:801–7. [DOI]
44. Ferro-Flores G, Arteaga de Murphy C, Rodriguez-Cortés J, Pedraza-López M, Ramírez-Iglesias MT. Preparation and evaluation of 99mTc-EDDA/HYNIC-[Lys 3]-bombesin for imaging gastrin-releasing peptide receptor-positive tumours. Nucl Med Commun. 2006;27:371–6. [DOI] [PubMed]
45. de Barros AL, Mota LD, Coelho MM, Corrêa NC, de Góes AM, Oliveira MC, et al. Bombesin Encapsulated in Long-Circulating pH-Sensitive Liposomes as a Radiotracer for Breast Tumor Identification. J Biomed Nanotechnol. 2015;11:342–50. [DOI] [PubMed]
46. Carlesso FN, Fuscaldi LL, Araújo RS, Teixeira CS, Oliveira MC, Fernandes SO, et al. Evaluation of ^{99m}Tc -HYNIC-βAla-Bombesin$_{(7-14)}$ as an agent for pancreas tumor detection in mice. Braz J Med Biol Res. 2015;48:923–8. [DOI] [PubMed] [PMC]
47. Fuscaldi LL, de Barros ALB, Santos CRP, de Oliveira MC, Fernandes SOA, Cardoso VN. Feasibility of the ^{99m}Tc-HYNIC-βAla-Bombesin$_{(7-14)}$ for detection of LNCaP prostate tumour in experimental model. J Radioanal Nucl Chem. 2015;305:379–86. [DOI]
48. Santos-Cuevas CL, Ferro-Flores G, Arteaga de Murphy C, Pichardo-Romero PA. Targeted imaging of gastrin-releasing peptide receptors with ^{99m}Tc-EDDA/HYNIC-[Lys^3]-bombesin: biokinetics and dosimetry in women. Nucl Med Commun. 2008;29:741–7. [DOI] [PubMed]
49. Faintuch B, Fernandez E, Teodoro R, Wiecek D, Agarbuio A, Moro A, et al. 99mTc-SAMA-GGG-Ahx-BBN for GRP receptor targeting. J Nucl Med. 2010;51:1527.
50. Faintuch BL, Oliveira EA, Nunez EG, Moro AM, Nanda PK, Smith CJ. Comparison of two peptide radiotracers for prostate carcinoma targeting. Clinics (Sao Paulo). 2012;67:163–70. [DOI] [PubMed] [PMC]
51. Zitzmann S, Mier W, Schad A, Kinscherf R, Askoxylakis V, Krämer S, et al. A new prostate carcinoma binding peptide (DUP-1) for tumor imaging and therapy. Clin Cancer Res. 2005;11:139–46. [PubMed]
52. Santos-Cuevas CL, Ferro-Flores G, Arteaga de Murphy C, Ramírez Fde M, Luna-Gutiérrez MA, Pedraza-López M, et al. Design, preparation, *in vitro* and *in vivo* evaluation of ^{99m}Tc-N_2S_2-Tat(49–57)-bombesin: a target-specific hybrid radiopharmaceutical. Int J Pharm. 2009;375:75–83. [DOI] [PubMed]
53. de Barros AL, Mota Ld, Ferreira Cde A, Oliveira MC, Góes AM, Cardoso VN. Bombesin derivative radiolabeled with technetium-99m as agent for tumor identification. Bioorg Med Chem Lett. 2010; 20:6182–4. [DOI] [PubMed]

54. Santos-Cuevas CL, Ferro-Flores G, Rojas-Calderón EL, García-Becerra R, Ordaz-Rosado D, Arteaga de Murphy C, et al. ^{99m}Tc-N_2S_2-Tat (49-57)-bombesin internalized in nuclei of prostate and breast cancer cells: kinetics, dosimetry and effect on cellular proliferation. Nucl Med Commun. 2011;32:303–13. [DOI] [PubMed]
55. de Barros AL, Mota Ld, Ferreira Cde A, Cardoso VN. Kit formulation for ^{99m}Tc-labeling of HYNIC-βAla-Bombesin$_{(7-14)}$. Appl Radiat Isot. 2012;70:2440–5. [DOI] [PubMed]
56. de Barros ALB, das Graças Mota L, de Aguiar Ferreira C, Corrêa NCR, de Góes AM, Oliveira MC, et al. ^{99m}Tc-labeled bombesin analog for breast cancer identification. J Radioanal Nucl Chem. 2013;295: 2083–90. [DOI]
57. Aranda-Lara L, Ferro-Flores G, Ramírez Fde M, Ocampo-García B, Santos-Cuevas C, Díaz-Nieto L, et al. Improved radiopharmaceutical based on ^{99m}Tc-Bombesin-folate for breast tumour imaging. Nucl Med Commun. 2016;37:377–86. [DOI] [PubMed]
58. Marostica LL, de Barros AL, Silva JO, Lopes SC, Salgado BS, Chondrogiannis S, et al. Feasibility study with ^{99m}Tc-HYNIC-βAla-Bombesin$_{(7-14)}$ as an agent to early visualization of lung tumour cells in nude mice. Nucl Med Commun. 2016;37:372–6. [DOI] [PubMed]
59. Ferreira CA, Fuscaldi LL, Townsend DM, Rubello D, Barros ALB. Radiolabeled bombesin derivatives for preclinical oncological imaging. Biomed Pharmacother. 2017;87:58–72. [DOI] [PubMed] [PMC]
60. Mendoza-Sánchez AN, Ferro-Flores G, Ocampo-García BE, Morales-Avila E, de M Ramírez F, De León-Rodríguez LM, et al. Lys^3-bombesin conjugated to ^{99m}Tc-labelled gold nanoparticles for *in vivo* gastrin releasing peptide-receptor imaging. J Biomed Nanotechnol. 2010;6:375–84. [DOI] [PubMed]
61. Jiménez-Mancilla N, Ferro-Flores G, Ocampo-García B, Luna-Gutiérrez M, De María Ramírez F, Pedraza-López M, et al. Multifunctional targeted radiotherapy system for induced tumours expressing gastrin-releasing peptide receptors. Curr Nanosci. 2012;8:193–201. [DOI]
62. Morales-Avila E, Ferro-Flores G, Ocampo-García BE, Gómez-Oliván LM. Engineered multifunctional RGD-gold nanoparticles for the detection of tumour-specific $\alpha(v)\beta(3)$ expression: chemical characterisation and ecotoxicological risk assessment. J Biomed Nanotechnol. 2012;8:991–9. [DOI] [PubMed]
63. de Barros AL, Mota Ld, Soares DC, de Souza CM, Cassali GD, Oliveira MC, et al. Long-circulating, pH-sensitive liposomes versus long-circulating, non-pH-sensitive liposomes as a delivery system for tumor identification. J Biomed Nanotechnol. 2013;9:1636–43. [DOI] [PubMed]
64. Jiménez-Mancilla N, Ferro-Flores G, Santos-Cuevas C, Ocampo-García B, Luna-Gutiérrez M, Azorín-Vega E, et al. Multifunctional targeted therapy system based on ^{99m}Tc/^{177}Lu-labeled gold nanoparticles-Tat(49–57)-Lys^3-bombesin internalized in nuclei of prostate cancer cells. J Labelled Comp Radiopharm. 2013;56:663–71. [DOI] [PubMed]
65. Stéen EJL, Edem PE, Nørregaard K, Jørgensen JT, Shalgunov V, Kjaer A, et al. Pretargeting in nuclear imaging and radionuclide therapy: Improving efficacy of theranostics and nanomedicines. Biomaterials. 2018;179:209–45. [DOI] [PubMed]
66. Verhoeven M, Seimbille Y, Dalm SU. Therapeutic Applications of Pretargeting. Pharmaceutics. 2019; 11:434. [DOI] [PubMed] [PMC]
67. Goodwin DA, Meares CF. Advances in pretargeting biotechnology. Biotechnol Adv. 2001;19:435–50. [DOI] [PubMed]
68. Warren TK, Shurtleff AC, Bavari S. Advanced morpholino oligomers: a novel approach to antiviral therapy. Antiviral Res. 2012;94:80–8. [DOI] [PubMed] [PMC]
69. Moulton JD, Yan YL. Using Morpholinos to control gene expression. Curr Protoc Mol Biol. 2008;83: 1–29. [DOI] [PubMed] [PMC]
70. Moulton JD. Using Morpholinos to Control Gene Expression. Curr Protoc Nucleic Acid Chem. 2017;68: 1–29. [DOI] [PubMed] [PMC]

71. Yeh SH, Lin CF, Kong FL, Wang HE, Hsieh YJ, Gelovani JG, et al. Molecular imaging of nonsmall cell lung carcinomas expressing active mutant EGFR kinase using PET with [^{124}i]-morpholino-IPQA. Biomed Res Int. 2013;2013:549359. [DOI] [PubMed] [PMC]
72. McCaffrey AP, Meuse L, Karimi M, Contag CH, Kay MA. A potent and specific morpholino antisense inhibitor of hepatitis C translation in mice. Hepatology. 2003;38:503–8. [DOI] [PubMed]
73. Faintuch BL, Núñez GE, Teodoro R, Moro AM, Mengatti J. Radiolabeled nano-peptides show specificity for an animal model of human PC3 prostate cancer cells. Clinics (Sao Paulo). 2011;66:327–36. [DOI] [PubMed] [PMC]
74. Brazeau P, Vale W, Burgus R, Ling N, Butcher M, Rivier J, et al. Hypothalamic polypeptide that inhibits the secretion of immunoreactive pituitary growth hormone. Science. 1973;179:77–9. [DOI] [PubMed]
75. Pittaluga A, Roggeri A, Vallarino G, Olivero G. Somatostatin, a Presynaptic Modulator of Glutamatergic Signal in the Central Nervous System. Int J Mol Sci. 2021;22:5864. [DOI] [PubMed] [PMC]
76. Molina Trinidad EM, Casas AS. Somatostatin analogs, how biomarkers in the diagnostic and treatment for cancer and others damages. Int J Pharm Sci Rev Res. 2014;27:31–46.
77. Gomes-Porras M, Cárdenas-Salas J, Álvarez-Escolá C. Somatostatin Analogs in Clinical Practice: a Review. Int J Mol Sci. 2020;21:1682. [DOI] [PubMed] [PMC]
78. de Jong M, Valkema R, Kwekkeboom DJ, Krenning EP. Somatostatin Receptor Targeted-Radio-Ablation of Tumors. Somatostatin. 2004:233–49. [DOI]
79. Faintuch BL, Pereira NPS, Faintuch S, Muramoto E, Silva CPG. Lanreotide and octreotide complexed with technetium-99m: labeling, stability and biodistribution studies. Rev Bras Cienc Farm. 2004;40:101–10.
80. Melo IB, Ueda LT, Araujo EB, Muramoto E, Barboz MF, Mengatti J, et al. Tecnetium-99m as alternative to produce somatostatin-labeled derivatives: Comparative biodistribution evaluation with 111In-DTPA-Octreotide. Cell Mol Biol. 2010;56:31–6.
81. Melero LTUH, Muramoto E, De Araújo EB. Preliminary studies of EDDA-tricine-HYNIC-Tyr^3-octreotide labelled with technetium-99m: radiopharmaceutical development for the diagnosis of neuroendocrine tumours. Atoms Peace. 2010;3:56–64. [DOI]
82. Ocampo-García B, Ferro-Flores G, Morales-Avila E, Ramírez Fde M. Kit for preparation of multimeric receptor-specific ^{99m}Tc-radiopharmaceuticals based on gold nanoparticles. Nucl Med Commun. 2011;32:1095–104. [DOI] [PubMed]
83. Orocio-Rodríguez E, Ferro-Flores G, Santos-Cuevas CL, Ramírez Fde M, Ocampo-García BE, Azorín-Vega E, et al. Two Novel Nanosized Radiolabeled Analogues of Somatostatin for Neuroendocrine Tumor Imaging. J Nanosci Nanotechnol. 2015;15:4159–69. [DOI] [PubMed]
84. Körner M, Christ E, Wild D, Reubi JC. Glucagon-like peptide-1 receptor overexpression in cancer and its impact on clinical applications. Front Endocrinol (Lausanne). 2012;3:158. [DOI] [PubMed] [PMC]
85. Reubi JC, Waser B. Concomitant expression of several peptide receptors in neuroendocrine tumours: molecular basis for in vivo multireceptor tumour targeting. Eur J Nucl Med Mol Imaging. 2003;30:781–93. [DOI] [PubMed]
86. Christ E, Wild D, Reubi JC. Glucagonlike peptide-1 receptor: an example of translational research in insulinomas: a review. Endocrinol Metab Clin North Am. 2010;39:791–800. [DOI] [PubMed]
87. Baggio LL, Drucker DJ. Biology of incretins: GLP-1 and GIP. Gastroenterology. 2007;132:2131–57. [DOI] [PubMed]
88. Manandhar B, Ahn JM. Glucagon-like peptide-1 (GLP-1) analogs: recent advances, new possibilities, and therapeutic implications. J Med Chem. 2015;58:1020–37. [DOI] [PubMed] [PMC]

89. Medina-García V, Ocampo-García BE, Ferro-Flores G, Santos-Cuevas CL, Aranda-Lara L, García-Becerra R, et al. A freeze-dried kit formulation for the preparation of Lys^{27}(^{99m}Tc-EDDA/HYNIC)-Exendin(9-39)/^{99m}Tc-EDDA/HYNIC-Tyr^{3}-Octreotide to detect benign and malignant insulinomas. Nucl Med Biol. 2015;42:911–6. [DOI] [PubMed]
90. Ocampo-García BE, Santos-Cuevas CL, Luna-Gutiérrez MA, Ignacio-Alvarez E, Pedraza-López M, Manzano-Mayoral C. ^{99m}Tc-exendin(9-39)/octreotide: biokinetics and radiation dosimetry in healthy individuals. Nucl Med Commun. 2017;38:912–8. [DOI] [PubMed]
91. Faintuch BL, Seo D, de Oliveira EA, Targino RC, Moro AM. Evaluation of the Influence of the Conjugation Site of the Chelator Agent HYNIC to GLP1 Antagonist Radiotracer for Insulinoma Diagnosis. Curr Radiopharm. 2017;10:65–72. [DOI] [PubMed]
92. Seo D, Faintuch BL, Aparecida de Oliveira E, Faintuch J. Pancreas and liver uptake of new radiolabeled incretins (GLP-1 and Exendin-4) in models of diet-induced and diet-restricted obesity. Nucl Med Biol. 2017;49:57–64. [DOI] [PubMed]
93. Plow EF, Haas TA, Zhang L, Loftus J, Smith JW. Ligand binding to integrins. J Biol Chem. 2000;275:21785–8. [DOI] [PubMed]
94. Jeschke B, Meyer J, Jonczyk A, Kessler H, Adamietz P, Meenen NM, et al. RGD-peptides for tissue engineering of articular cartilage. Biomaterials. 2002;23:3455–63. [DOI] [PubMed]
95. Gaertner FC, Kessler H, Wester HJ, Schwaiger M, Beer AJ. Radiolabelled RGD peptides for imaging and therapy. Eur J Nucl Med Mol Imaging. 2012;39:S126–38. [DOI] [PubMed]
96. Santulli G, Basilicata MF, De Simone M, Del Giudice C, Anastasio A, Sorriento D, et al. Evaluation of the anti-angiogenic properties of the new selective $\alpha_v\beta_3$ integrin antagonist RGDechiHCit. J Transl Med. 2011;9:7. [DOI] [PubMed] [PMC]
97. Chen K, Chen X. Integrin targeted delivery of chemotherapeutics. Theranostics. 2011;1:189–200. [DOI] [PubMed] [PMC]
98. Leonidis G, Dalezis P, Trafalis D, Beis D, Giardoglou P, Koukiali A, et al. Synthesis and Biological Evaluation of a c(RGDyK) Peptide Conjugate of SRPIN803. ACS Omega. 2021;6:28379–93. [DOI] [PubMed] [PMC]
99. Decristoforo C, Faintuch-Linkowski B, Rey A, von Guggenberg E, Rupprich M, Hernandez-Gonzales I, et al. [^{99m}Tc]HYNIC-RGD for imaging integrin $\alpha_v\beta_3$ expression. Nucl Med Biol. 2006;33:945–52. [DOI] [PubMed]
100. Inoue Y, Yoshikawa K, Yoshioka N, Watanabe T, Saegusa S, Kaneko Y, et al. Evaluation of renal function with ^{99m}Tc-MAG3 using semiautomated regions of interest. J Nucl Med. 2000;41:1947–54. [PubMed]
101. Piepsz A, Tondeur M, Ham H. Relative ^{99m}Tc-MAG3 renal uptake: reproducibility and accuracy. J Nucl Med. 1999;40:972–6. [PubMed]
102. de Oliveira EA, Faintuch B, Fernández Núñez EG, Santos RP, da Silva N, Targino R, et al. ^{99m}Tc-MAG3-PEG8-c(RGDYK) uptake in melanoma tumor. J Nucl Med. 2011;52.
103. Oliveira ÉA, Faintuch BL, Núñez EGF, Maria Moro A, Nanda PK, Smith CJ. Radiotracers for different angiogenesis receptors in a melanoma model. Melanoma Res. 2012;22:45–53. [DOI]
104. Faintuch BL, Oliveira EA, Targino RC, Moro AM. Radiolabeled NGR phage display peptide sequence for tumor targeting. Appl Radiat Isot. 2014;86:41–5. [DOI] [PubMed]
105. Däpp S, García Garayoa E, Maes V, Brans L, Tourwé DA, Müller C, et al. PEGylation of ^{99m}Tc-labeled bombesin analogues improves their pharmacokinetic properties. Nucl Med Biol. 2011;38:997–1009. [DOI] [PubMed]
106. Schiper L, Faintuch BL, Badaró RJ, Oliveira EA, Chavez VE, Chinen E, et al. Functional investigation of bone implant viability using radiotracers in a new model of osteonecrosis. Clinics (Sao Paulo). 2016;71:617–25. [DOI] [PubMed] [PMC]

107. Morales-Avila E, Ferro-Flores G, Ocampo-García BE, De León-Rodríguez LM, Santos-Cuevas CL, García-Becerra R, et al. Multimeric system of ^{99m}Tc-labeled gold nanoparticles conjugated to c[RGDfK(C)] for molecular imaging of tumor α(v)β(3) expression. Bioconjug Chem. 2011;22:913–22. [DOI] [PubMed]
108. Haubner R, Gratias R, Diefenbach B, Goodman SL, Jonczyk A, Kessler H. Structural and Functional Aspects of RGD-Containing Cyclic Pentapeptides as Highly Potent and Selective Integrin $\alpha_v\beta_3$ Antagonists. J Am Chem Soc. 1996;118:7461–72. [DOI]
109. Calderan A, Biondi B, Bolzati C, Refosco F, Morellato N, Salvarese N, et al. Synthesis, in vitro and in vivo evaluation of new 99mTc-labeled cyclic RGDfK peptide monocationic complexes. J Peptide Sci. 2012;18:S157–8.
110. Caporale A, Bolzati C, Incisivo GM, Salvarese N, Grieco P, Ruvo M. Improved synthesis on solid phase of dithiocarbamic cRGD-derivative and ^{99m}Tc-radiolabelling. J Pept Sci. 2019;25:e3140. [DOI] [PubMed]
111. Lei Z, Chai N, Tian M, Zhang Y, Wang G, Liu J, et al. Novel peptide GX1 inhibits angiogenesis by specifically binding to transglutaminase-2 in the tumorous endothelial cells of gastric cancer. Cell Death Dis. 2018;9:579. [DOI] [PubMed] [PMC]
112. Zhi M, Wu KC, Dong L, Hao ZM, Deng TZ, Hong L, et al. Characterization of a specific phage-displayed Peptide binding to vasculature of human gastric cancer. Cancer Biol Ther. 2004;3:1232–5. [DOI] [PubMed]
113. Dijkgraaf I, Kruijtzer JA, Liu S, Soede AC, Oyen WJ, Corstens FH, et al. Improved targeting of the $\alpha_v\beta_3$ integrin by multimerisation of RGD peptides. Eur J Nucl Med Mol Imaging. 2007;34:267–73. [DOI] [PubMed]
114. Oliveira EA, Faintuch BL. Radiolabeling and biological evaluation of the GX1 and RGD-GX1 peptide sequence for angiogenesis targeting. Nucl Med Biol. 2015;42:123–30. [DOI] [PubMed]
115. de Oliveira ÉA, Faintuch BL, Seo D, Barbezan AB, Funari A, Targino RC, et al. Radiolabeled GX1 Peptide for Tumor Angiogenesis Imaging. Appl Biochem Biotechnol. 2018;185:863–74. [DOI]
116. de Oliveira ÉA, Faintuch BL, Targino RC, Moro AM, Martinez RCR, Pagano RL, et al. Evaluation of GX1 and RGD-GX1 peptides as new radiotracers for angiogenesis evaluation in experimental glioma models. Amino Acids. 2016;48:821–31. [DOI]
117. de Oliveira EA, Lazovic J, Guo L, Soto H, Faintuch BL, Akhtari M, et al. Evaluation of Magnetonanoparticles Conjugated with New Angiogenesis Peptides in Intracranial Glioma Tumors by MRI. Appl Biochem Biotechnol. 2017;183:265–79. [DOI] [PubMed]
118. Sobral DV, Fuscaldi LL, Durante ACR, Mendonça FF, de Oliveira LR, Miranda ACC, et al. Comparative Evaluation of Radiochemical and Biological Properties of ^{131}I- and [^{99m}Tc]Tc$(CO)_3$-Labeled RGD Analogues Planned to Interact with the $\alpha_v\beta_3$ Integrin Expressed in Glioblastoma. Pharmaceuticals (Basel). 2022;15:116. [DOI] [PubMed] [PMC]
119. Friry C, Feliciangeli S, Richard F, Kitabgi P, Rovere C. Production of recombinant large proneurotensin/neuromedin N-derived peptides and characterization of their binding and biological activity. Biochem Biophys Res Commun. 2002;290:1161–8. [DOI] [PubMed]
120. St-Gelais F, Jomphe C, Trudeau L. The role of neurotensin in central nervous system pathophysiology: what is the evidence? J Psychiatry Neurosci. 2006;31:229–45. [PubMed] [PMC]
121. Binder EB, Kinkead B, Owens MJ, Nemeroff CB. Neurotensin and dopamine interactions. Pharmacol Rev. 2001;53:453–86. [PubMed]
122. García-Garayoa E, Maes V, Bläuenstein P, Blanc A, Hohn A, Tourwé D, et al. Double-stabilized neurotensin analogues as potential radiopharmaceuticals for NTR-positive tumors. Nucl Med Biol. 2006;33:495–503. [DOI] [PubMed]
123. Teodoro R, Faintuch BL, Núñez EG, Queiróz RG. Neurotensin(8–13) analogue: radiolabeling and biological evaluation using different chelators. Nucl Med Biol. 2011;38:113–20. [DOI] [PubMed]

124. Santos DM, Verly RM, Piló-Veloso D, de Maria M, de Carvalho MA, Cisalpino PS, et al. LyeTx I, a potent antimicrobial peptide from the venom of the spider *Lycosa erythrognatha*. Amino Acids. 2010;39: 135–44. [DOI] [PubMed]
125. Vieira APGC, de Souza AN, Lima WG, Brito JCM, Simião DC, Gonçalves LVR, et al. The Synthetic Peptide LyeTx I mnΔK, Derived from *Lycosa erythrognatha* Spider Toxin, Is Active against Methicillin-Resistant *Staphylococcus aureus* (MRSA) In Vitro and In Vivo. Antibiotics (Basel). 2024; 13:248. [DOI] [PubMed] [PMC]
126. César Moreira Brito J, Gustavo Lima W, Magalhães Resende J, Cristina Sampaio de Assis D, Boff D, Nascimento Cardoso V, et al. Pegylated LyeTx I-b peptide is effective against carbapenem-resistant *Acinetobacter baumannii* in an *in vivo* model of pneumonia and shows reduced toxicity. Int J Pharm. 2021;609:121156. [DOI] [PubMed]
127. Fuscaldi LL, Dos Santos DM, Pinheiro NG, Araújo RS, de Barros AL, Resende JM, et al. Synthesis and antimicrobial evaluation of two peptide LyeTx I derivatives modified with the chelating agent HYNIC for radiolabeling with technetium-99m. J Venom Anim Toxins Incl Trop Dis. 2016;22:16. [DOI] [PubMed] [PMC]
128. Fuscaldi LL, de Avelar Júnior JT, Dos Santos DM, Boff D, de Oliveira VLS, Gomes KAGG, et al. Shortened derivatives from native antimicrobial peptide LyeTx I: *In vitro* and *in vivo* biological activity assessment. Exp Biol Med (Maywood). 2021;246:414–25. [DOI] [PubMed] [PMC]
129. Ferreira IM, de Sousa Lacerda CM, Dos Santos SR, de Barros ALB, Fernandes SO, Cardoso VN, et al. Detection of bacterial infection by a technetium-99m-labeled peptidoglycan aptamer. Biomed Pharmacother. 2017;93:931–8. [DOI] [PubMed]
130. Ferro-Flores G, Ocampo-Garcia BE, Melendez-Alafort L. Development of specific radio-pharmaceuticals for infection imaging by targeting infectious micro-organisms. Curr Pharm Des. 2012;18:1098–106. [DOI] [PubMed]
131. Auletta S, Baldoni D, Varani M, Galli F, Hajar IA, Duatti A, et al. Comparison of 99mTc-UBI 29-41, 99mTc-ciprofloxacin, 99mTc-ciprofloxacin dithiocarbamate and 111In-biotin for targeting experimental Staphylococcus aureus and Escherichia coli foreign-body infections: an ex-vivo study. Q J Nucl Med Mol Imaging. 2019;63:37–47. [DOI] [PubMed]
132. Signore A, Artiko V, Conserva M, Ferro-Flores G, Welling MM, Jain SK, et al. Imaging Bacteria with Radiolabelled Probes: Is It Feasible? J Clin Med. 2020;9:2372. [DOI] [PubMed] [PMC]
133. Marjanovic-Painter B, Kleynhans J, Zeevaart JR, Rohwer E, Ebenhan T. A decade of ubiquicidin development for PET imaging of infection: A systematic review. Nucl Med Biol. 2023;116–117: 108307. [DOI] [PubMed]
134. Ferro-Flores G, de María Ramírez F, Meléndez-Alafort L, de Murphy CA, Pedraza-López M. Molecular recognition and stability of ^{99m}Tc-UBI 29–41 based on experimental and semiempirical results. Appl Radiat Isot. 2004;61:1261–8. [DOI] [PubMed]
135. Ferro-Flores G, Arteaga de Murphy C, Palomares-Rodríguez P, Meléndez-Alafort L, Pedraza-López M. Kit for instant ^{99m}Tc labeling of the antimicrobial peptide ubiquicidin 29-41. J Radioanal Nucl Chem. 2005;266:307–11. [DOI]
136. Sepúlveda-Méndez J, de Murphy CA, Rojas-Bautista JC, Pedraza-López M. Specificity of ^{99m}Tc-UBI for detecting infection foci in patients with fever in study. Nucl Med Commun. 2010;31:889–95. [DOI] [PubMed]
137. Meléndez-Alafort L, Rodríguez-Cortés J, Ferro-Flores G, Arteaga De Murphy C, Herrera-Rodríguez R, Mitsoura E, et al. Biokinetics of ^{99m}Tc-UBI 29-41 in humans. Nucl Med Biol. 2004;31:373–9. [DOI] [PubMed]
138. Vallejo E, Martinez I, Tejero A, Hernandez S, Jimenez L, Bialostozky D, et al. Clinical utility of ^{99m}Tc-labeled ubiquicidin 29–41 antimicrobial peptide for the scintigraphic detection of mediastinitis after cardiac surgery. Arch Med Res. 2008;39:768–74. [DOI] [PubMed]

139. Sathekge M, Garcia-Perez O, Paez D, El-Haj N, Kain-Godoy T, Lawal I, et al. Molecular imaging in musculoskeletal infections with ^{99m}Tc-UBI 29-41 SPECT/CT. Ann Nucl Med. 2018;32:54–9. [DOI] [PubMed]
140. Flores-Vázquez JG, Rodriguez-Hernandez LA, Becerril-Vega G, Rodríguez-Hernández IA, Eguiluz-Melendez AG, Suarez-Rivera O. Technetium-99m-ubiquicidin 29-41 SPECT-CT to detect postsurgical spinal infection: A case report. Surg Neurol Int. 2024;15:24. [DOI] [PubMed] [PMC]